

# Amplitude analysis of electroproduction data

A. Sarantsev

NRC 'Kurchatov Institute' PNPI, Gatchina



Petersburg  
Nuclear  
Physics  
Institute

StrongQCD VI, Nanjing University, 14-17 May 2024

# Energy dependent fully covariant approach

In many cases an unambiguous partial wave decomposition at fixed energies is impossible. Then the energy and angular parts should be analyzed together:

$$A(s, t) = \sum_{\beta\beta'n} A_n^{\beta\beta'}(s) Q_{\mu_1 \dots \mu_n}^{(\beta)+} F_{\nu_1 \dots \nu_n}^{\mu_1 \dots \mu_n} Q_{\nu_1 \dots \nu_n}^{(\beta')}$$

$\pi N$  interaction:

$$Q_{\mu_1 \dots \mu_n}^{(+n)} = X_{\mu_1 \dots \mu_n}^{(n)} \quad Q_{\mu_1 \dots \mu_n}^{(-n)} = i\gamma_\nu \gamma_5 X_{\nu \mu_1 \dots \mu_n}^{(n+1)}$$

$$X^0 = 1; \quad X_\mu^1 = k_\mu^\perp; \quad X_{\mu\nu}^2 = \frac{3}{2} \left( k_\mu^\perp k_\nu^\perp - \frac{1}{3} k_\perp^2 g_{\mu\nu}^\perp \right);$$

$$X_{\mu\nu\alpha}^3 = \frac{5}{2} \left[ k_\mu^\perp k_\nu^\perp k_\alpha^\perp - \frac{k_\perp^2}{5} (g_{\mu\nu}^\perp k_\alpha^\perp + g_{\mu\alpha}^\perp k_\nu^\perp + g_{\nu\alpha}^\perp k_\mu^\perp) \right],$$

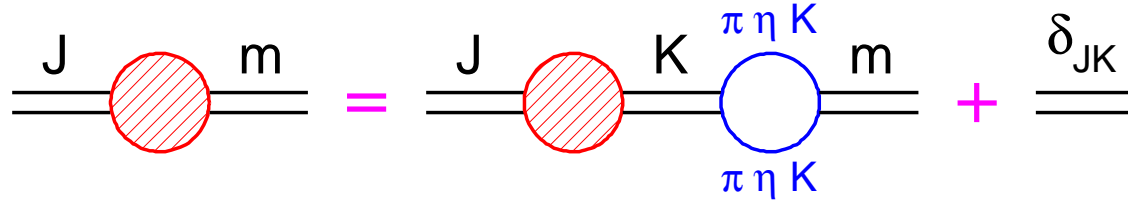
1. C. Zemach, Phys. Rev. 140, B97 (1965); 140, B109 (1965).

2. S.U.Chung, Phys. Rev. D 57, 431 (1998).

A. V. Anisovich, V. V. Anisovich, V. N. Markov, M. A. Matveev and A. V. Sarantsev, J. Phys. G 28, 15 (2002)

3. B. S. Zou and D. V. Bugg, Eur. Phys. J. A 16, 537 (2003)

# N/D based (D-matrix) coupled channel analysis of the data



$$D_{jm} = D_{jk} \sum_{\alpha} B_{\alpha}^{km}(s) \frac{1}{M_m - s} + \frac{\delta_{jm}}{M_j^2 - s} \quad \hat{D} = \hat{\kappa}(I - \hat{B}\hat{\kappa})^{-1}$$

$$\hat{\kappa} = \text{diag} \left( \frac{1}{M_1^2 - s}, \frac{1}{M_2^2 - s}, \dots, \frac{1}{M_N^2 - s}, R_1, R_2 \dots \right)$$

$$\hat{B}_{ij} = \sum_{\alpha} B_{\alpha}^{ij} = \sum_{\alpha} \int \frac{ds'}{\pi} \frac{g_{\alpha}^{(R)i} \rho_{\alpha}(s', m_{1\alpha}, m_{2\alpha}) g_{\alpha}^{(L)j}}{s' - s - i0}$$

**Channels included in D-matrix:**  $\pi N, \eta N, K\Lambda, K\Sigma, \Delta\pi, N\sigma, N(1685)\pi, N\rho(770), N\omega$  **and Black Box.**

$$A_{\alpha\beta} = g_{\alpha}^{(R)j} \hat{D}_{ji} g_{\beta}^{(L)i}$$

In the present fits we calculate the elements of the  $B_\alpha^{ij}$  using one subtraction taken at the channel threshold  $M_\alpha = (m_{1\alpha} + m_{2\alpha})$ :

$$B_\alpha^{ij}(s) = B_\alpha^{ij}(M_\alpha^2) + (s - M_\alpha^2) \int_{M_\alpha^2}^{\infty} \frac{ds'}{\pi} \frac{g_\alpha^{(R)i} \rho_\alpha(s', m_{1\alpha}, m_{2\alpha}) g_\alpha^{(L)j}}{(s' - s - i0)(s' - M_\alpha^2)}.$$

In this case the expression for elements of the  $\hat{B}$  matrix can be rewritten as:

$$B_\alpha^{ij}(s) = g_a^{(R)i} \left( b^\alpha + (s - M_\alpha^2) \int_{M_\alpha^2}^{\infty} \frac{ds'}{\pi} \frac{\rho_\alpha(s', m_{1\alpha}, m_{2\alpha})}{(s' - s - i0)(s' - M_\alpha^2)} \right) g_\beta^{(L)j} = g_a^{(R)i} B_\alpha g_\beta^{(L)j}$$

and D-matrix method equivalent to the K-matrix method with loop diagram with real part taken into account:

$$A = \hat{K}(I - \hat{B}\hat{K})^{-1} \quad B_{\alpha\beta} = \delta_{\alpha\beta} B_\alpha$$

## Meson photo-production and electro-production data

$$A_\alpha = P_\alpha + P_j B_{ij} \hat{\kappa}_j (I - \hat{B} \hat{\kappa})_{jm}^{-1} g_\alpha^{(L)m}$$

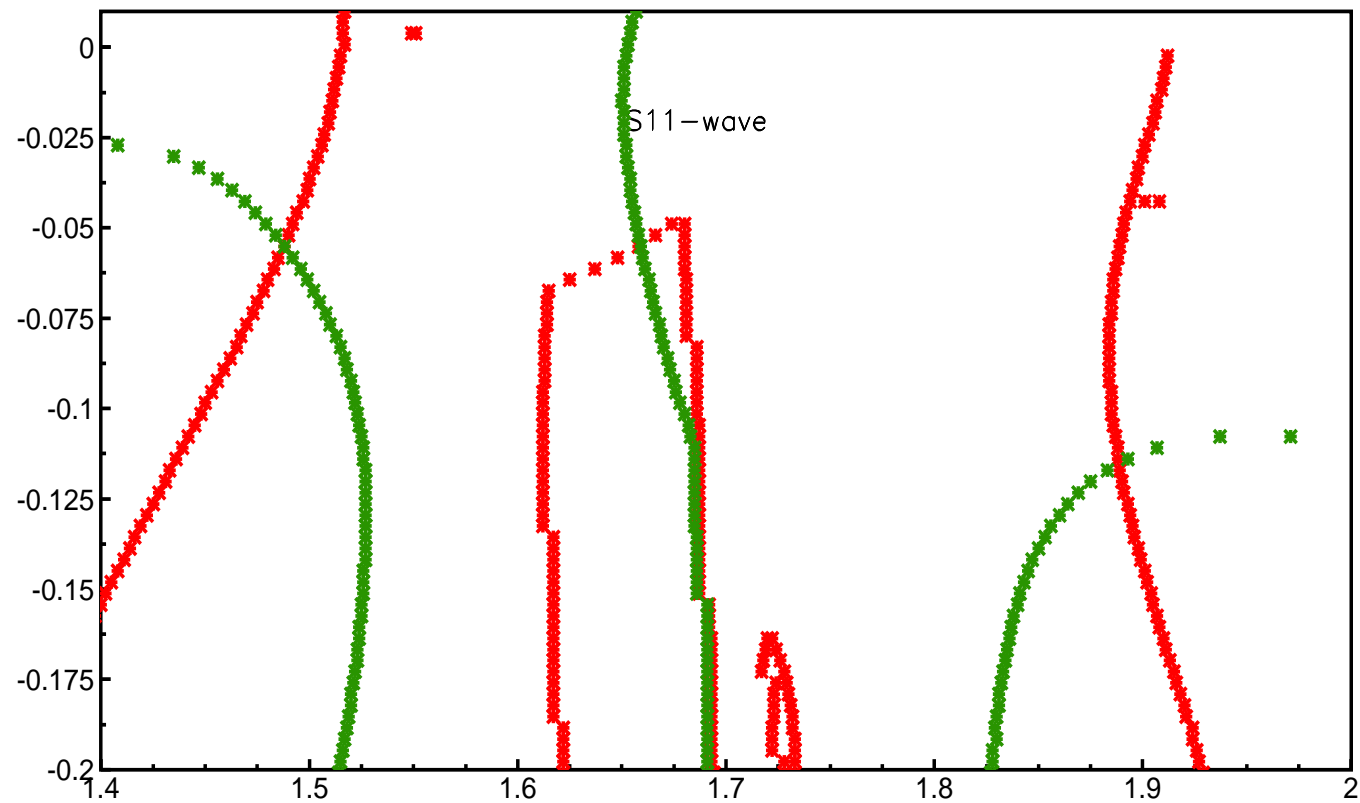
where

$$P_\alpha = \left( \frac{\Lambda_1 g_\alpha^{(R)1}}{M_1^2 - s}, \frac{\Lambda_2 g_\alpha^{(R)2}}{M_2^2 - s}, \dots, \frac{\Lambda_N g_\alpha^{(R)N}}{M_N^2 - s}, F_1, F_2 \dots \right)$$

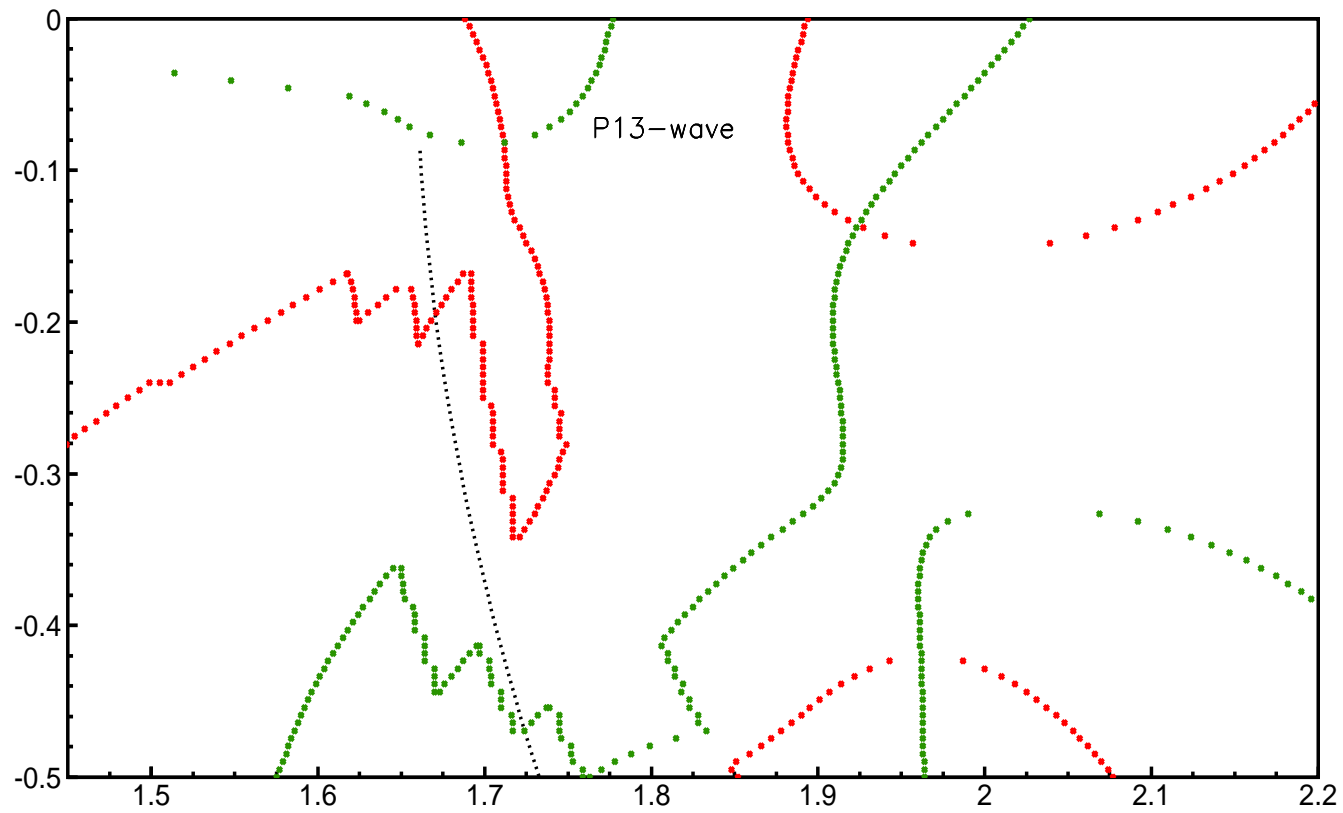
## The zero-trajectories of the denominator of the amplitude

$$DEN(s) = \det(I - \hat{B}\hat{K}) \prod_{i=1}^N (M_i^2 - s)$$

for the  $S_{11}$  partial wave



# The zero-trajectories of the denominator of the amplitude for the $P_{13}$ partial wave



## The included meson photoproduction data

DATA	2011-2019	added in 2020-2024
$\pi N \rightarrow \pi N$ ampl. $\pi^- p \rightarrow \pi \pi N$ $\pi^- p \rightarrow \eta n$ $\pi p \rightarrow K \Lambda, K \Sigma$ $\pi p \rightarrow \omega n$	<b>SAID</b> $d\sigma/d\Omega$ ( $\pi^0 \pi^0 n, \pi^+ \pi^- n, \pi^- \pi^0 p$ ) $d\sigma/d\Omega$ $d\sigma/d\Omega, P, \beta$	<b>Hoehler (energy fixed)</b>    $d\sigma/d\Omega$
$\gamma p \rightarrow \pi N$ $\gamma p \rightarrow \eta p$ $\gamma p \rightarrow \eta' p$	$d\sigma/d\Omega, \Sigma, T, P, E, G, H$ ( $\pi^0 p, \pi^+ n$ ) $d\sigma/d\Omega, \Sigma, F, T, P, H, G, E$ $d\sigma/d\Omega, \Sigma$	
$\gamma p \rightarrow K \Lambda, K \Sigma$	$d\sigma/d\Omega, \Sigma, P, T, C_x, C_z, O_{x'}, O_{z'}, T_x, T_z$	
$\gamma p \rightarrow \pi^0 \pi^0 p$ $\gamma p \rightarrow \pi^+ \pi^- p$	$d\sigma/d\Omega, \Sigma, E, I_c, I_s$ $d\sigma/d\Omega I_c, I_s$	$\Sigma, E, T, P, H, F, P_x, P_y$ $d\sigma/d\Omega(2.4 \text{ GeV}) P_x, P_y$ ( <b>CLAS</b> )
$\gamma p \rightarrow \omega p$	$d\sigma/d\Omega, \Sigma, \rho_{ij}^k, E, G$ ( <b>CB-ELSA</b> ), $\Sigma, P, T, F, H$ ( <b>CLAS</b> )	<b>Taken explicitly</b>
$\gamma n \rightarrow \Lambda K, \Sigma^- K$ $\gamma n \rightarrow \pi^- p$ $\gamma n \rightarrow \eta n$ $\gamma n \rightarrow \pi^0 n$	$d\sigma/d\Omega$ ( <b>CLAS</b> ), <b>E (CLAS)</b> $d\sigma/d\Omega, \Sigma, P, E, \Sigma$ ( <b>CLAS</b> ) $d\sigma/d\Omega$ ( <b>CB-ELSA, MAMI</b> ), $\Sigma, d\sigma/d\Omega$ ( $h = \frac{1}{2}$ ) ( <b>CB-ELSA</b> )	$\Sigma, G$ ( <b>CLAS</b> )    $d\sigma/d\Omega$

# Minimization methods

1. The two body final states  $\pi N, \gamma N \rightarrow \pi N, \eta N, K \Lambda, K \Sigma, \omega N, K^* \Lambda$ :  $\chi^2$  method.

For  $n$  measured bins we minimize

$$\chi^2 = \sum_j^n \frac{(\sigma_j(PWA) - \sigma_j(exp))^2}{(\Delta\sigma_j(exp))^2}$$

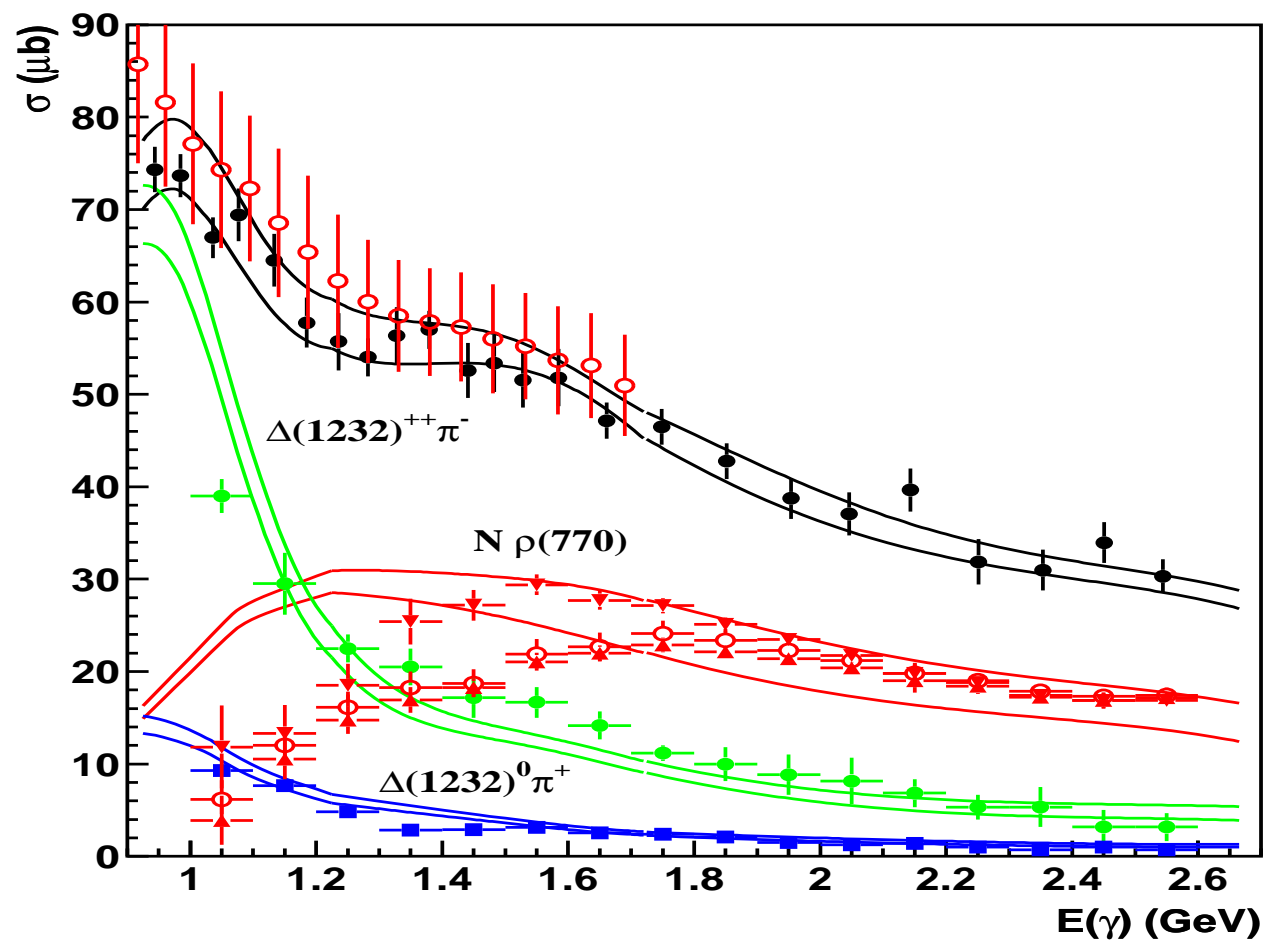
Present solution for  $\gamma p$  reaction  $\chi^2 = 69435$  for 46644 points.  $\chi^2/N_F = 1.49$

2. Reactions with three or more final states are analyzed with logarithm likelihood method.  $\pi N, \gamma N \rightarrow \pi\pi N, \pi\eta N$ . The minimization function:

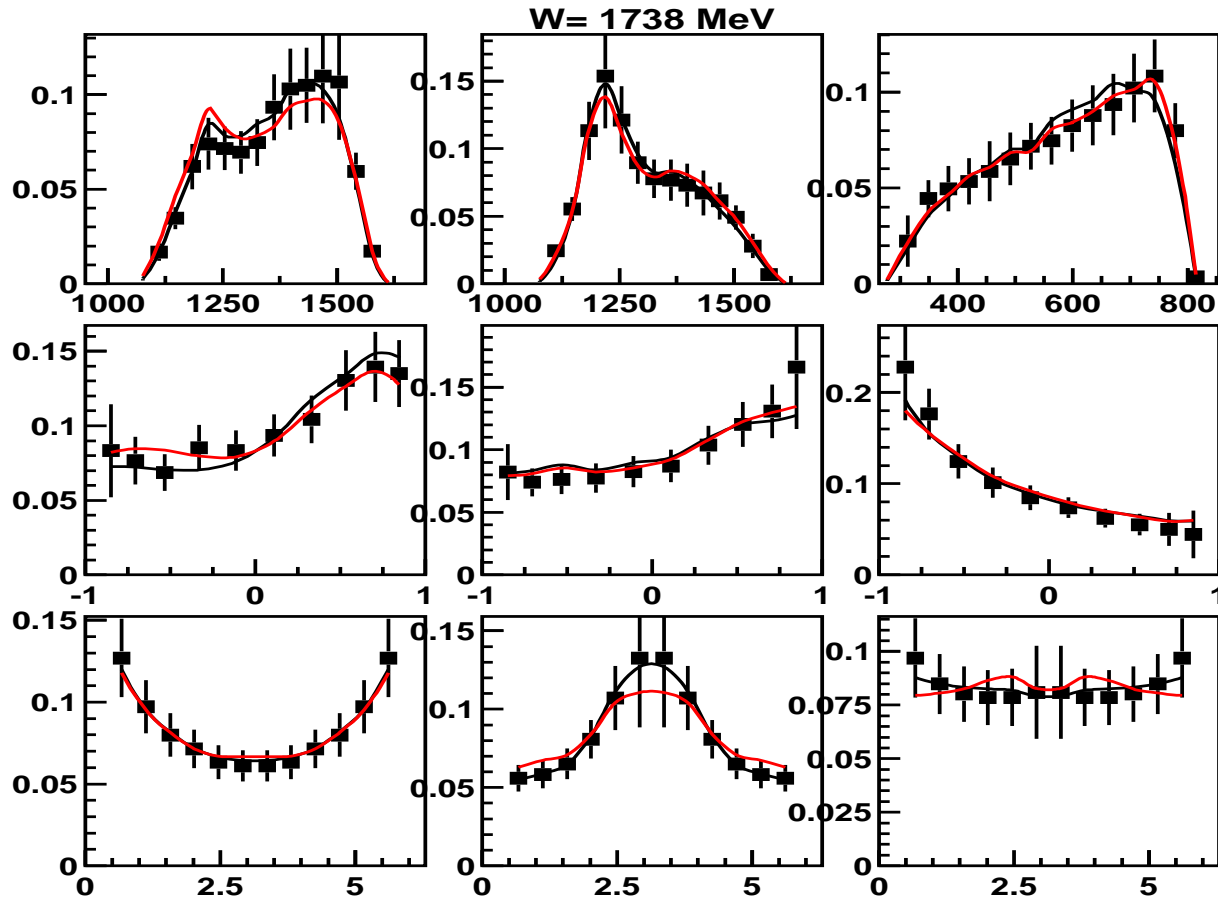
$$f = - \sum_j^{N(data)} \ln \frac{\sigma_j(PWA)}{\sum_m^{N(rec MC)} \sigma_m(PWA)}$$

This method allows us to take into account all correlations in many dimensional phase space. Above 1 000 000 data events are taken in the fit.

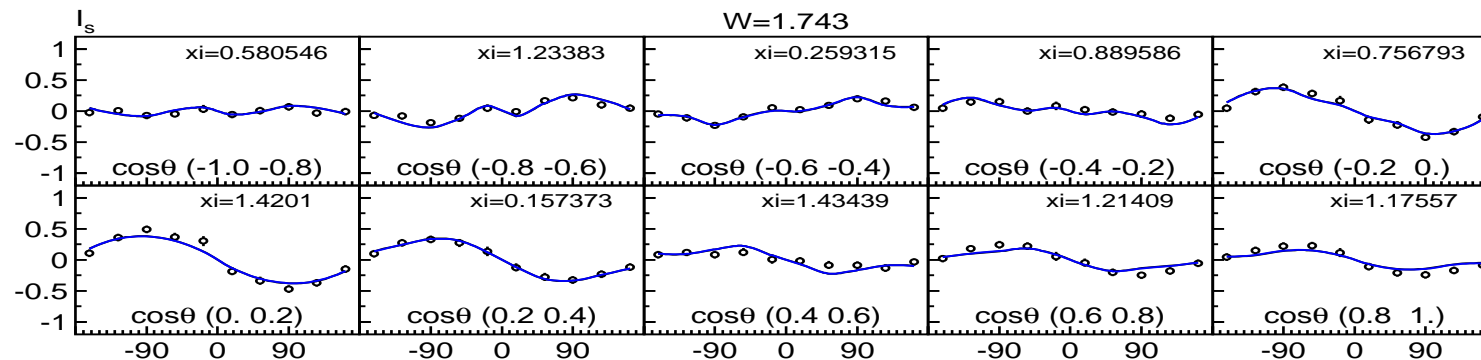
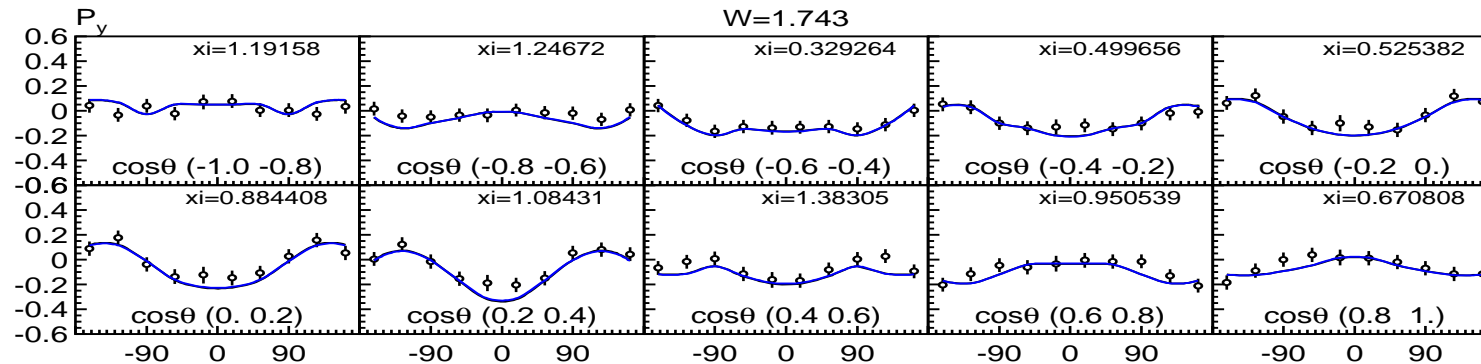
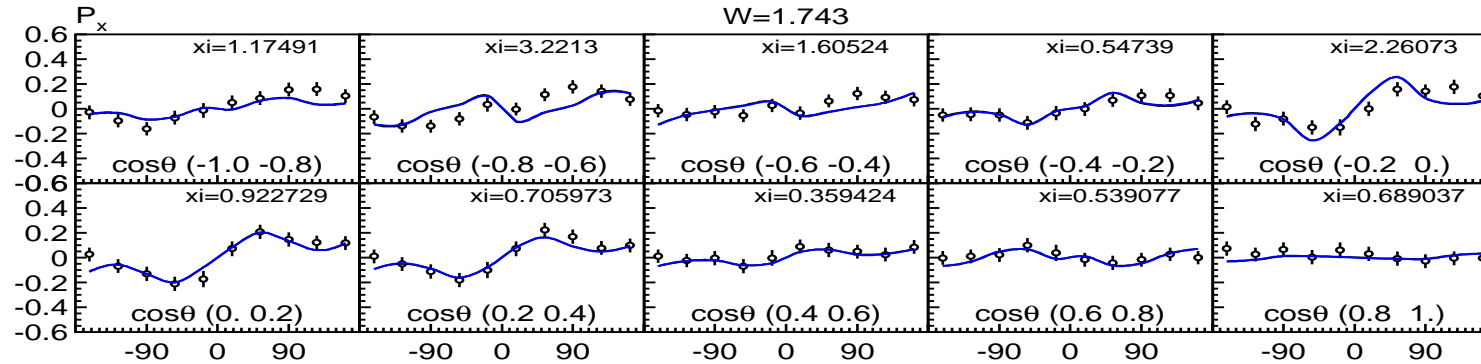
The fit of the CLAS data on  $\gamma p \rightarrow \pi^+ \pi^- p$ . The acceptance corrected data are shown



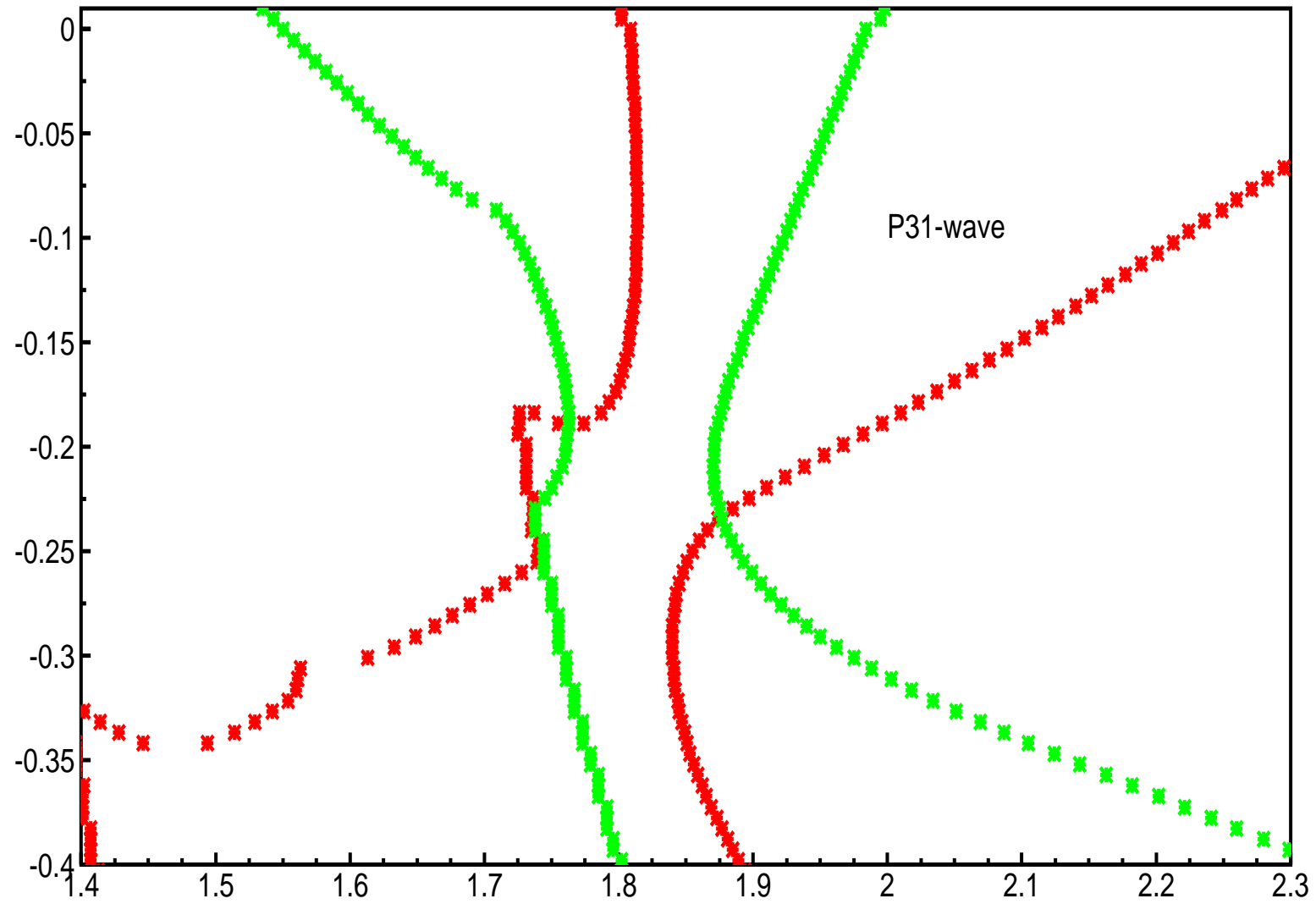
The comparison of the results obtained with fit of the 9-one dimensional projections and maximum likelihood method for the  $\gamma p \rightarrow \pi^+ \pi^- p$ . The acceptance corrected data are shown



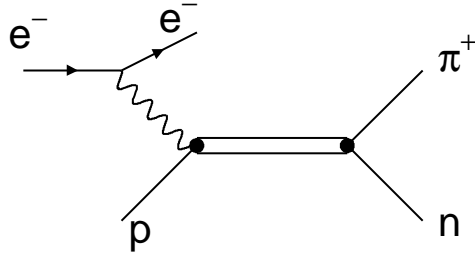
It seems that including polarization data needs indicate the presence of the structure in  
the  $P_{31}$  partial wave



The zero-trajectories of the denominator of the amplitude for the  $P_{31}$  partial wave



## Electro-production of pseudoscalar mesons



$$A = \omega^* J_\mu \omega' \bar{u}(k_f) \gamma_\mu u(k_i) \frac{e}{q^2}$$

$$|A|^2 = J_\mu J_\nu^* \frac{e^2}{2Q^4} \left( 2K_\mu K_\nu + \frac{q^2}{2} g_{\mu\nu} - \frac{1}{2} q_\mu q_\nu + ih \varepsilon_{\mu\nu\alpha\beta} q_\alpha K_\beta \right)$$

$$\frac{d\sigma}{d\Omega_f d\varepsilon_f d\Omega_\pi} = \Gamma \frac{d\sigma_v}{d\Omega_\pi} \quad \Gamma = \frac{\alpha}{2\pi^2} \frac{\varepsilon_f}{\varepsilon_i} \frac{|k_\gamma|}{Q^2} \frac{1}{1-\varepsilon}$$

$$\begin{aligned} \frac{d\sigma_v}{d\Omega_\pi} &= \frac{d\sigma_T}{d\Omega_\pi} + \varepsilon_L \frac{d\sigma_L}{d\Omega_\pi} + [2\varepsilon_L(1+\varepsilon)]^{\frac{1}{2}} \frac{d\sigma_{TL}}{d\Omega_\pi} \cos \Phi_\pi + \varepsilon \frac{d\sigma_{TT}}{d\Omega_\pi} \cos 2\Phi_\pi \\ &+ h [2\varepsilon_L(1-\varepsilon)]^{\frac{1}{2}} \frac{d\sigma_{TL'}}{d\Omega_\pi} + h(1-\varepsilon^2)^{\frac{1}{2}} \frac{d\sigma_{TT'}}{d\Omega_\pi} \end{aligned}$$

$\varepsilon_i, k_i, \varepsilon_f, k_f$  - momenta of the initial and final electrons ( $K = \frac{1}{2}(k_i + k_f)$ ).  $\vec{q}$  and  $\Theta_e$  are evaluated in the lab. frame.  $h$  is the helicity of the incoming electron. [Amaldi et al 1979](#), [Donnachie and Shaw 1978](#)

### The included meson electro-production data

<b>DATA</b>	<b>Mass range (MeV)</b>	<b><math>Q^2</math>-range (GeV<sup>2</sup>)</b>	<b>Observables</b>
$\gamma p \rightarrow \pi^0 p$	<b>1160-1340</b>	<b>0.16-0.32</b>	$\sigma_{TeL}, \sigma_{TL}, \sigma_{TT}$
$\gamma p \rightarrow \pi^0 p$	<b>1160-1790</b>	<b>0.4-0.90</b>	$\sigma_{TeL}, \sigma_{TL}, \sigma_{TT}, \text{Phi}$
$\gamma p \rightarrow \pi^+ n$	<b>1160-1340</b>	<b>0.16-0,32</b>	$\sigma_{TeL}, \sigma_{TL}, \sigma_{TT}$
$\gamma p \rightarrow \pi^+ n$	<b>1160-1680</b>	<b>0.3-0.6</b>	$\sigma_{TeL}, \sigma_{TL}, \sigma_{TT}$
$\gamma p \rightarrow \eta p$	<b>1500-1740</b>	<b>0.3,0.80</b>	$\sigma_{TeL}, \sigma_{TL}, \sigma_{TT}$
$\gamma p \rightarrow K \Lambda$	<b>1600-1850</b>	<b>0.65,1.0</b>	$\sigma_{TeL}, \sigma_{TL}, \sigma_{TT}$

## Siegert theorem

The behavior of the multipoles at physical threshold (pion momentum  $\vec{q} \rightarrow 0$ ) and pseudothreshold (Siegert limit, photon momentum  $\vec{k} \rightarrow 0$ ) is connected due to gauge invariance. It imposes the following model-independent relations:

$$(E_{L+}^I, L_{L+}^I) \rightarrow k^L q^L \quad (L \geq 0) \quad (1)$$

$$(M_{L+}^I, M_{L-}^I) \rightarrow k^L q^L \quad (L \geq 1) \quad (2)$$

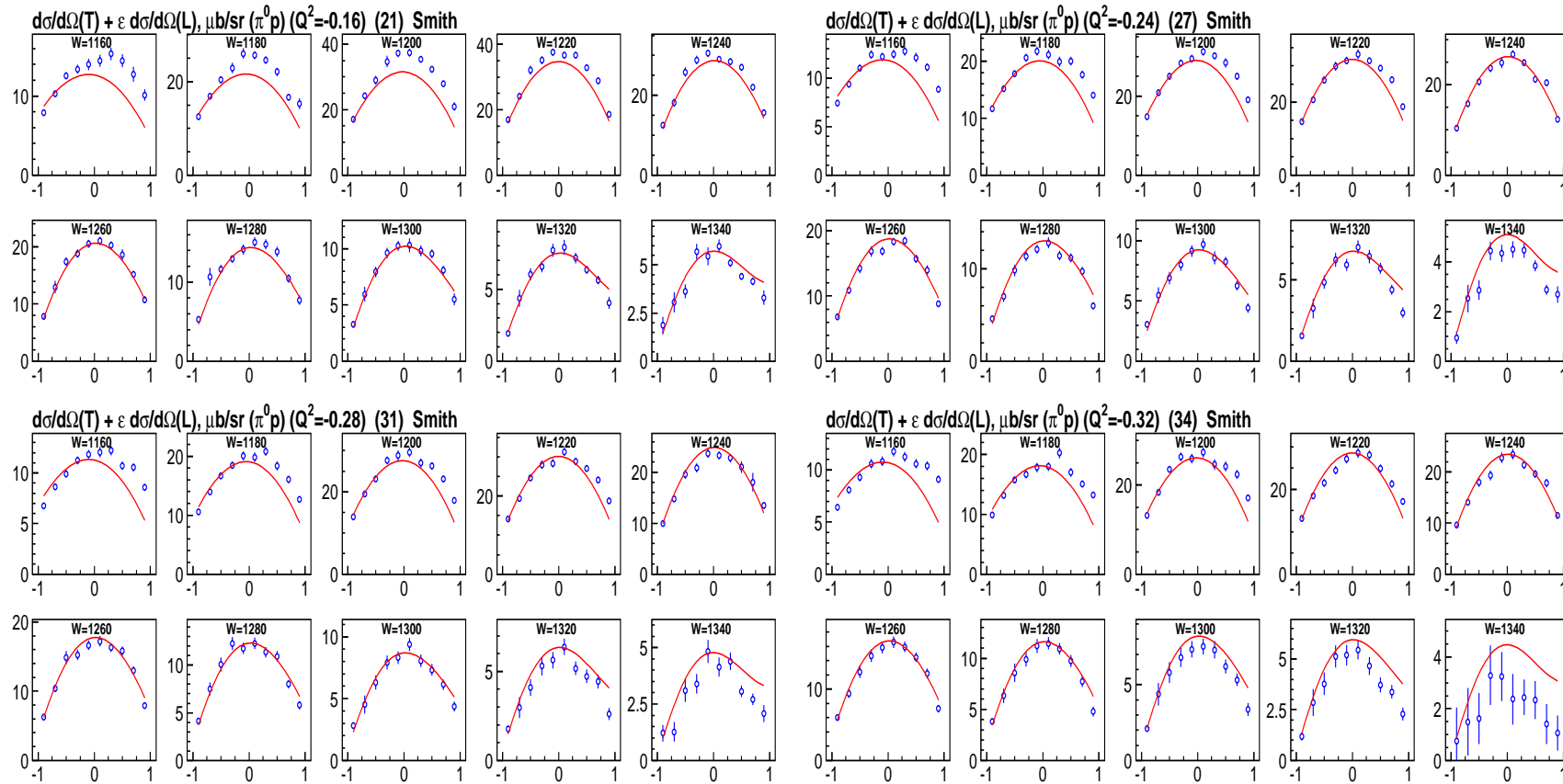
$$(L_{L-}^I) \rightarrow kq \quad (L = 1) \quad (3)$$

$$(E_{L-}^I, L_{L-}^I) \rightarrow k^{L-2} q^L \quad (L \geq 2)$$

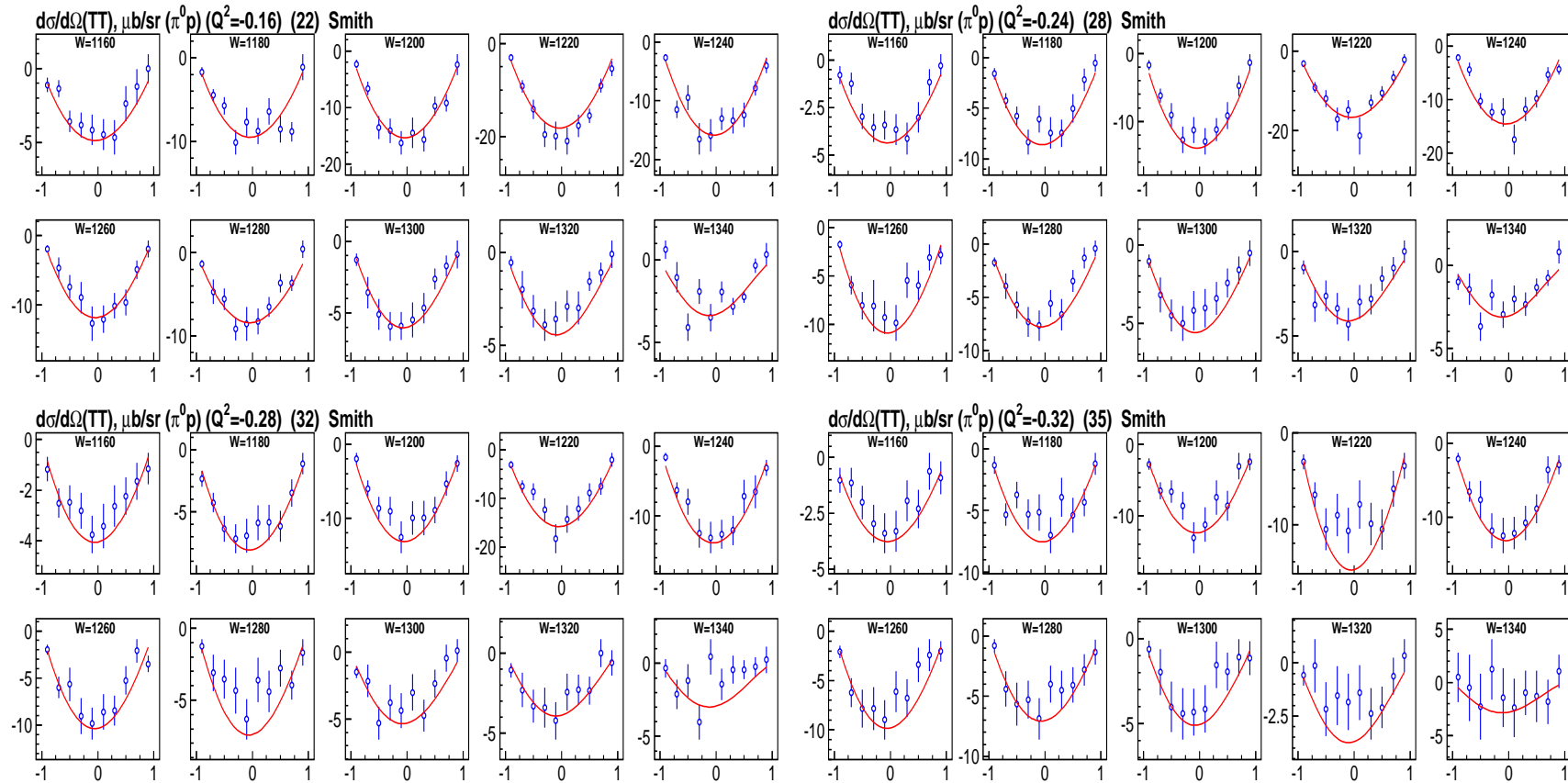
At  $Q^2 = -(W - m)^2$  because of no direction is defined for  $\vec{k} = 0$ , the electric and longitudinal multipoles are no longer independent.

$$E_{L+}^I / L_{L+}^I \rightarrow 1 \quad \text{and} \quad E_{L-}^I / L_{L-}^I \rightarrow -L / (L - 1) \quad k \rightarrow 0$$

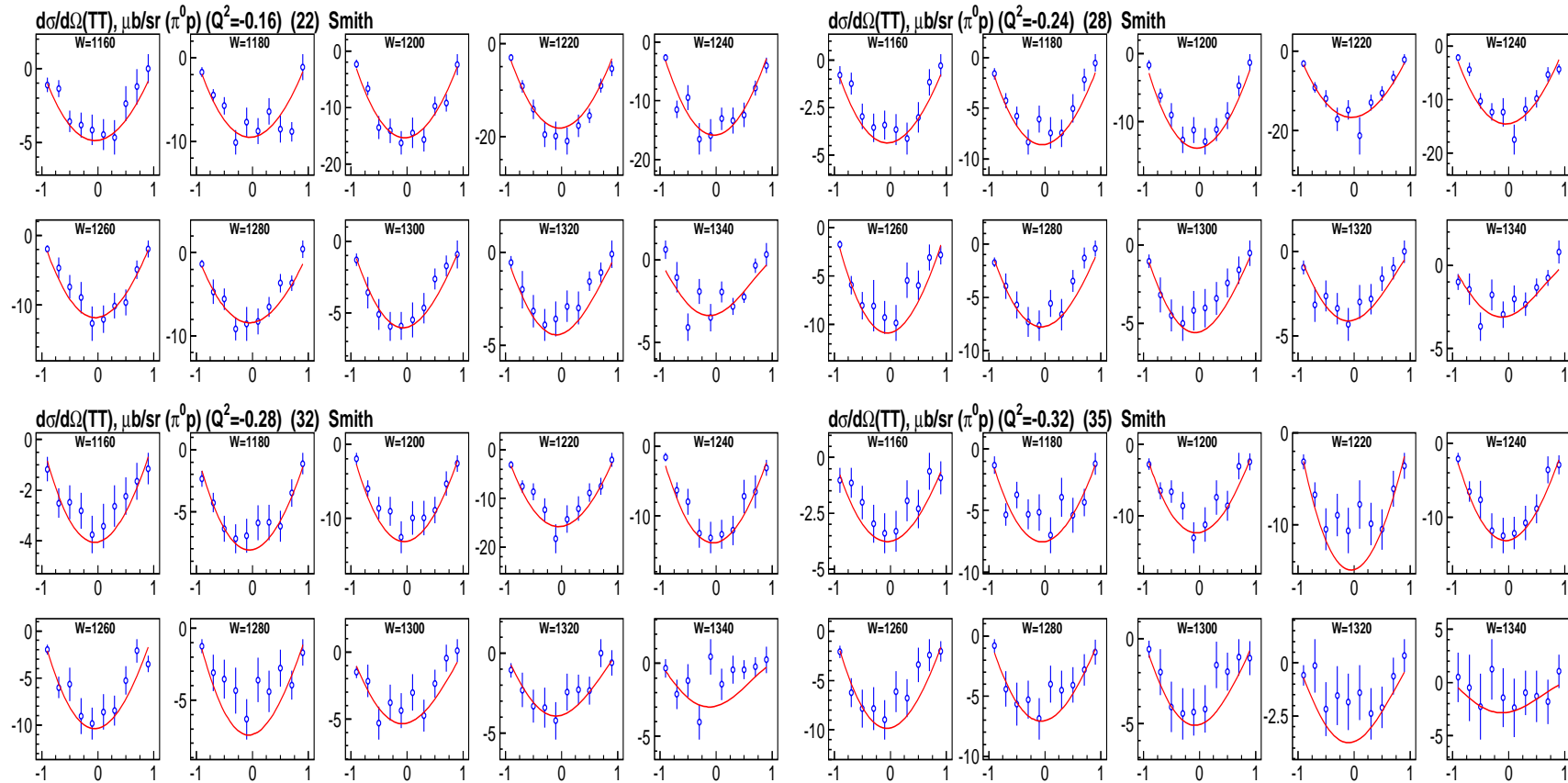
## The description of the $\gamma^* p \rightarrow \pi^0 p$ data



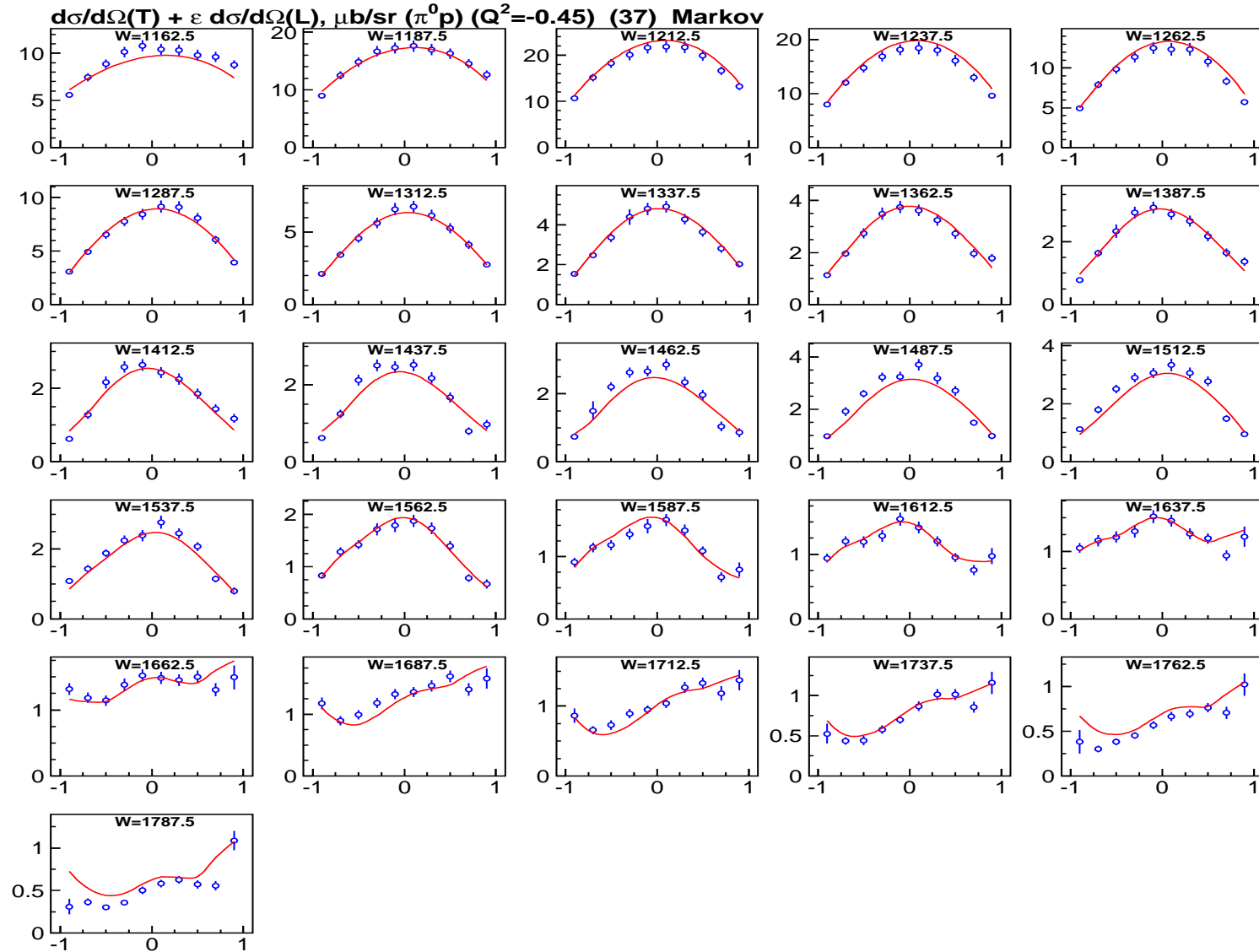
# The description of the $\gamma^* p \rightarrow \pi^0 p$ data



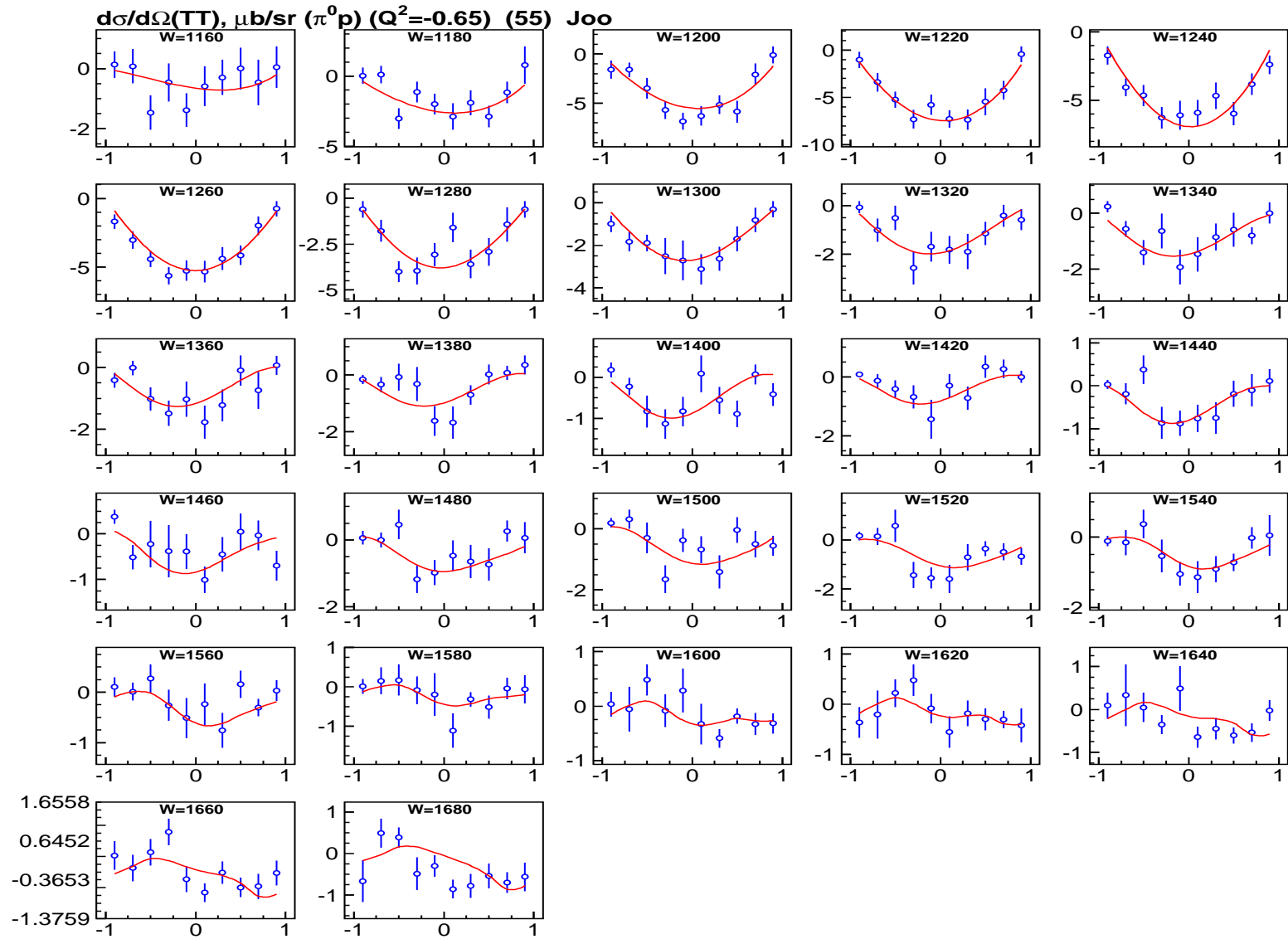
# The description of the $\gamma^* p \rightarrow \pi^0 p$ data



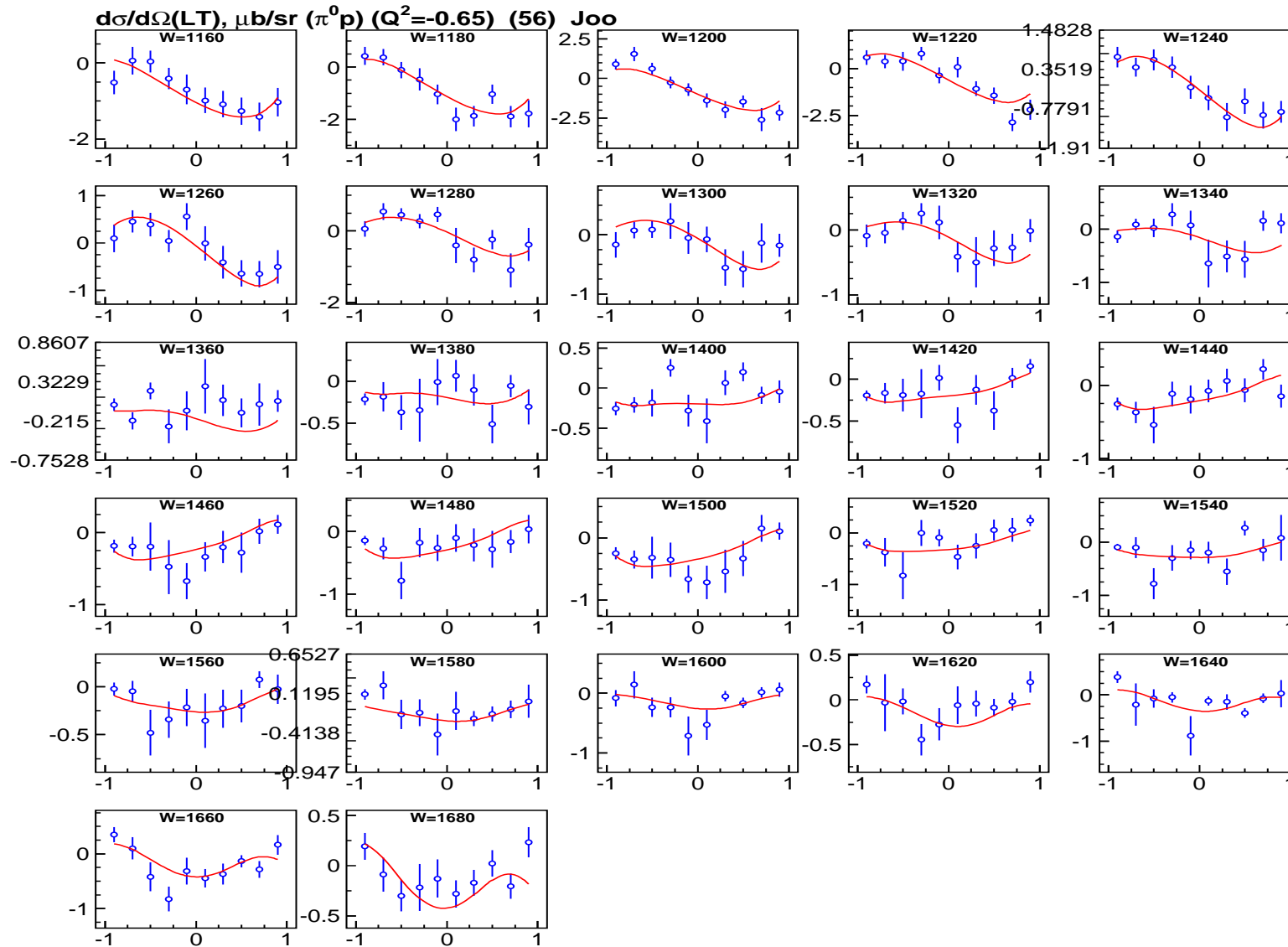
# The description of the $\gamma^* p \rightarrow \pi^0 p$ data



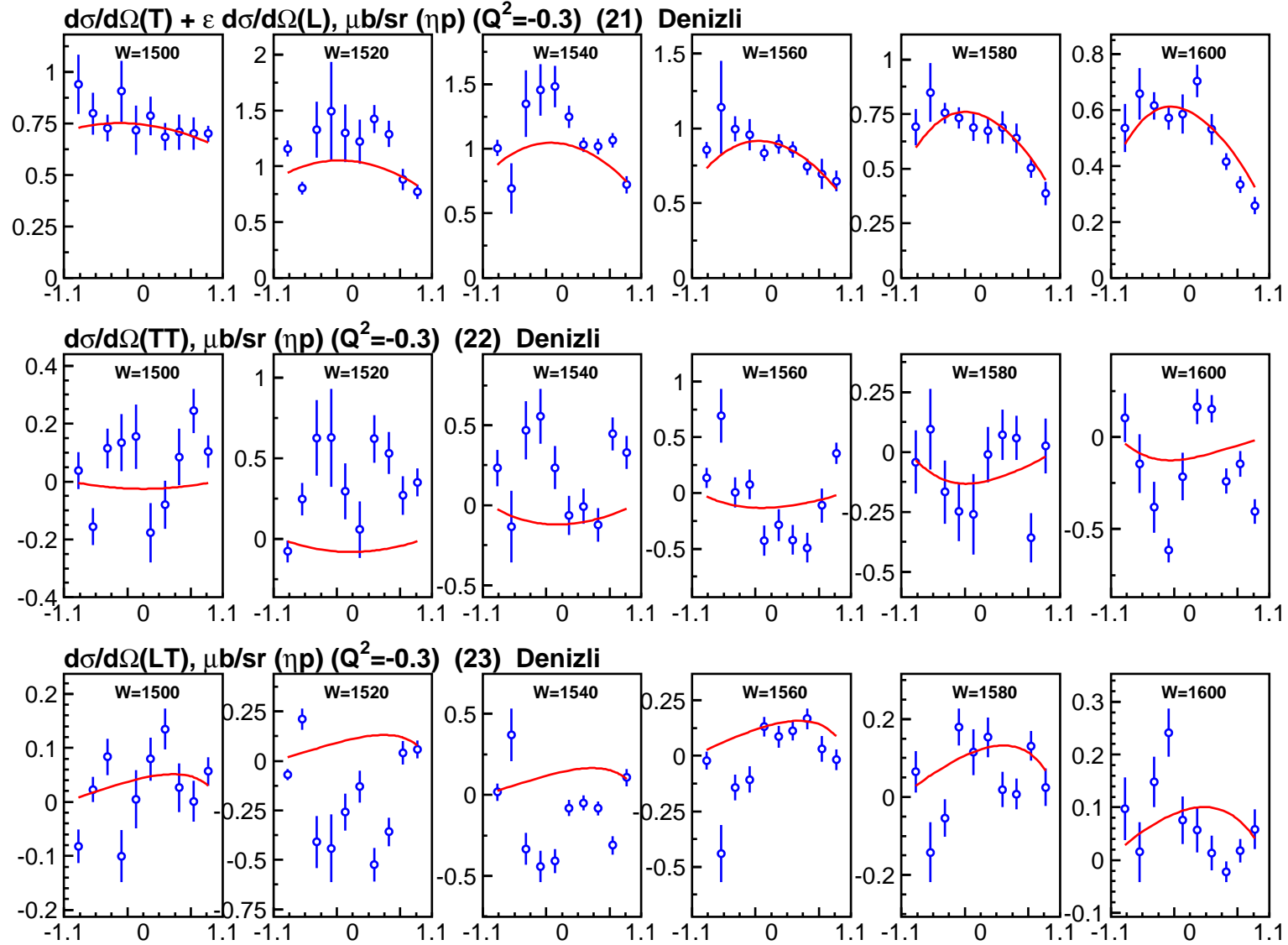
# The description of the $\gamma^* p \rightarrow \pi^0 p$ data



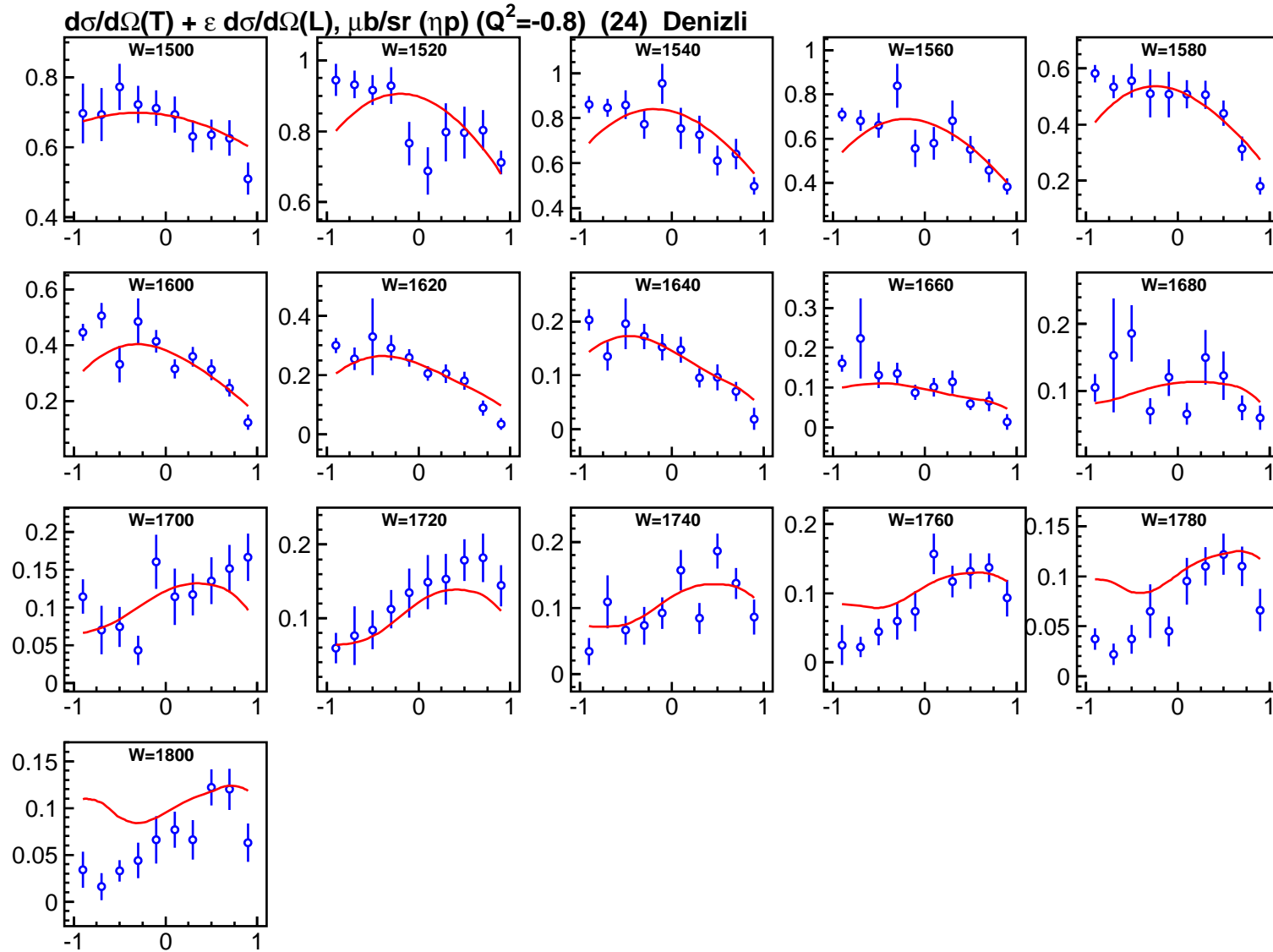
# The description of the $\gamma^* p \rightarrow \pi^0 p$ data



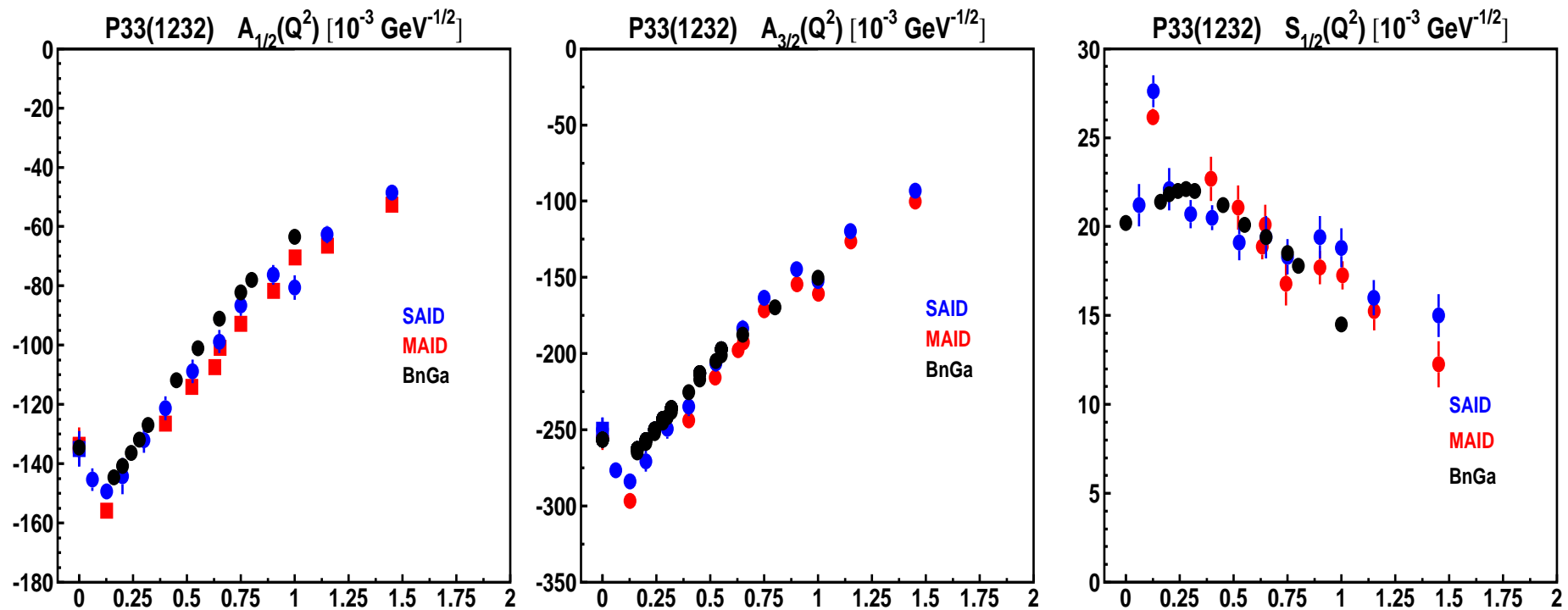
## The description of the $\gamma^* p \rightarrow \eta p$ data



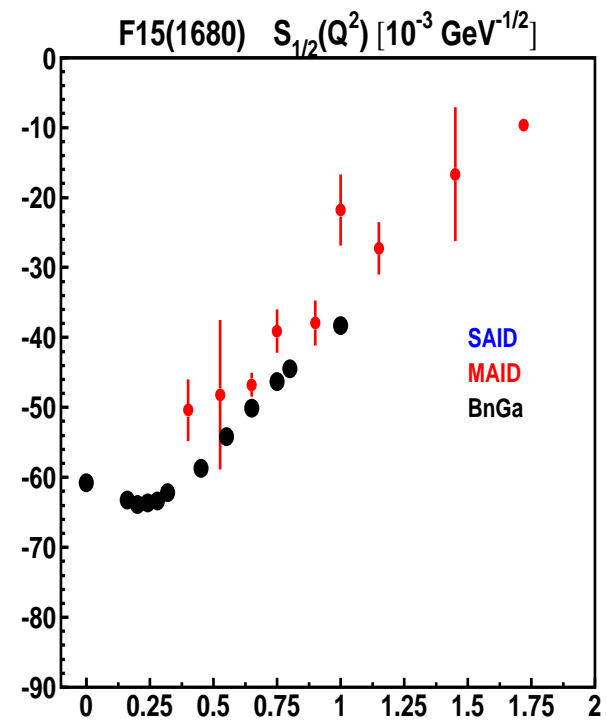
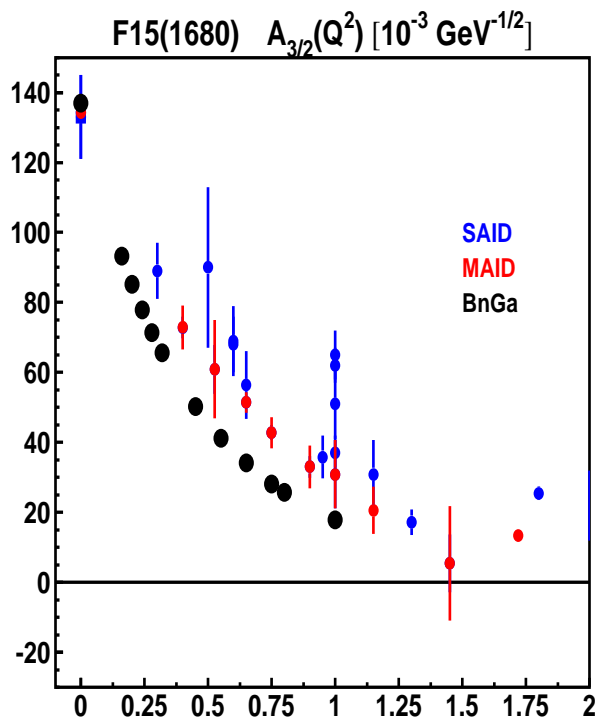
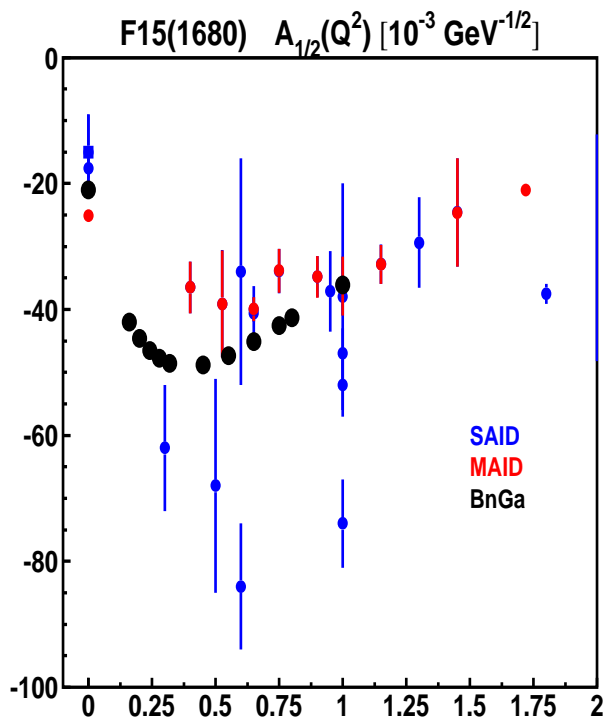
# The description of the $\gamma^* p \rightarrow \eta p$ data



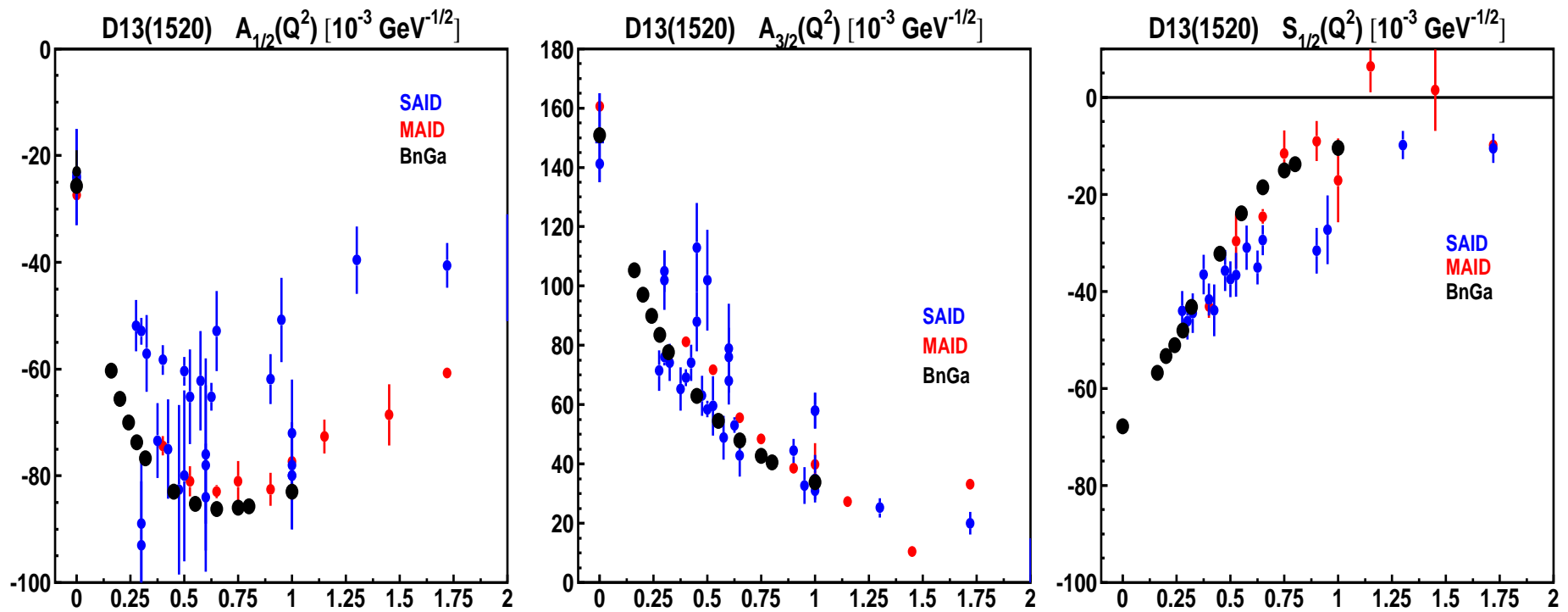
## The form factors for the $P_{33}(1232)$ state



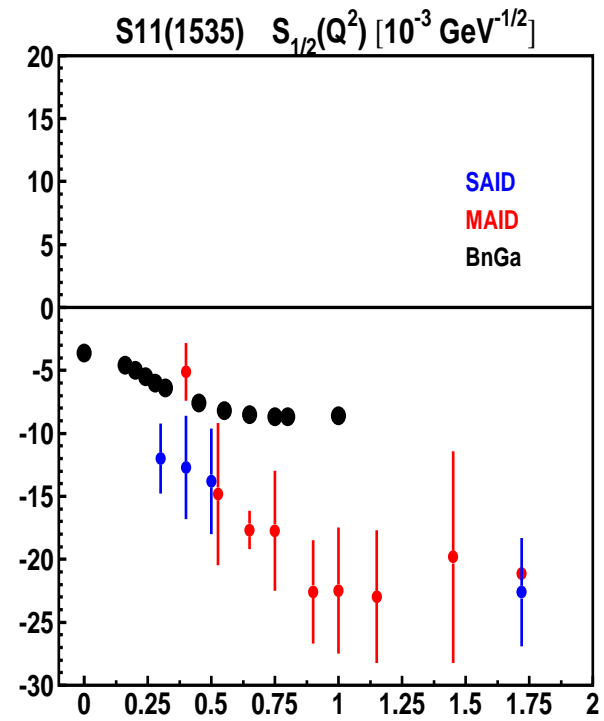
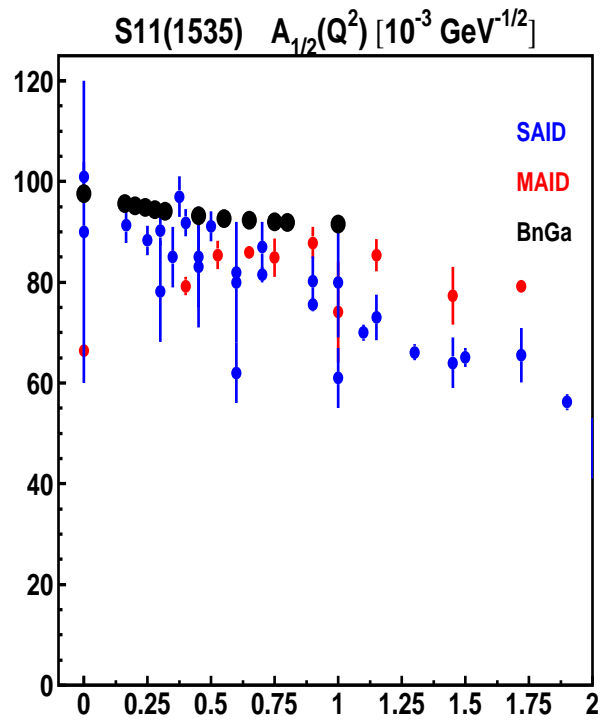
## The form factors for the $F_{15}(1680)$ state



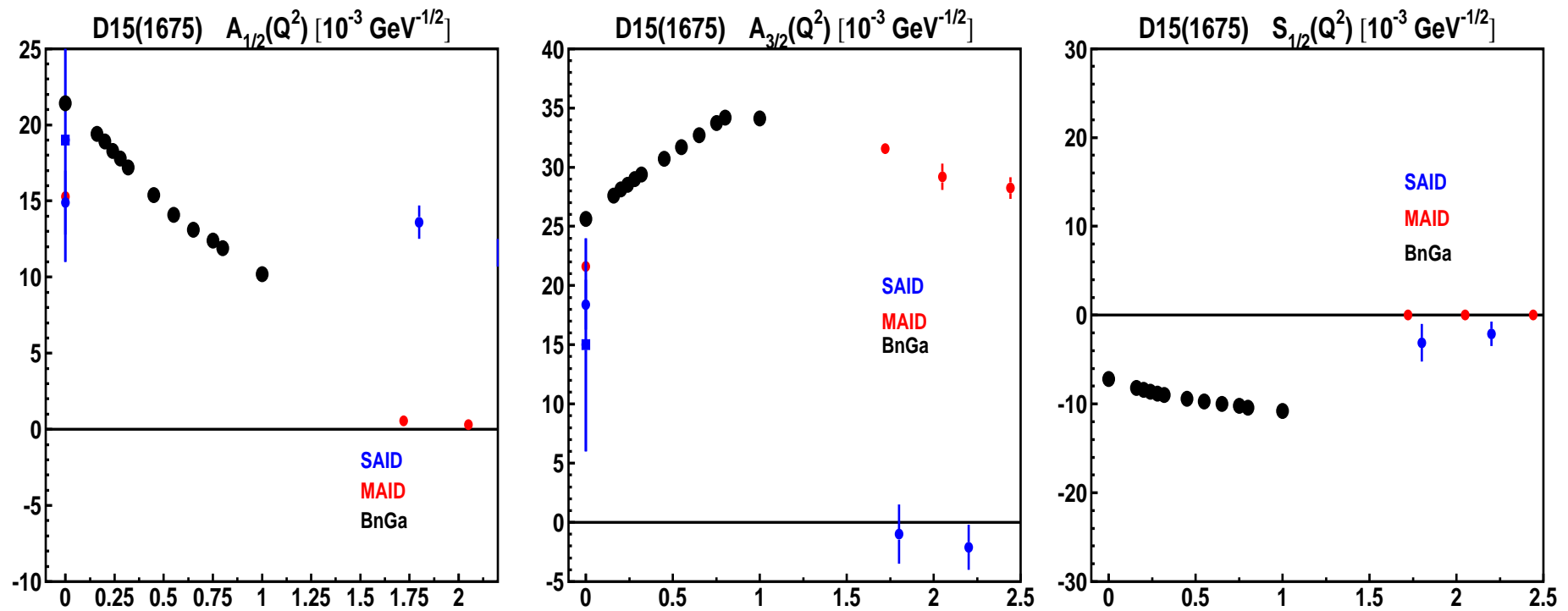
## The form factors for the $D_{13}(1520)$ state



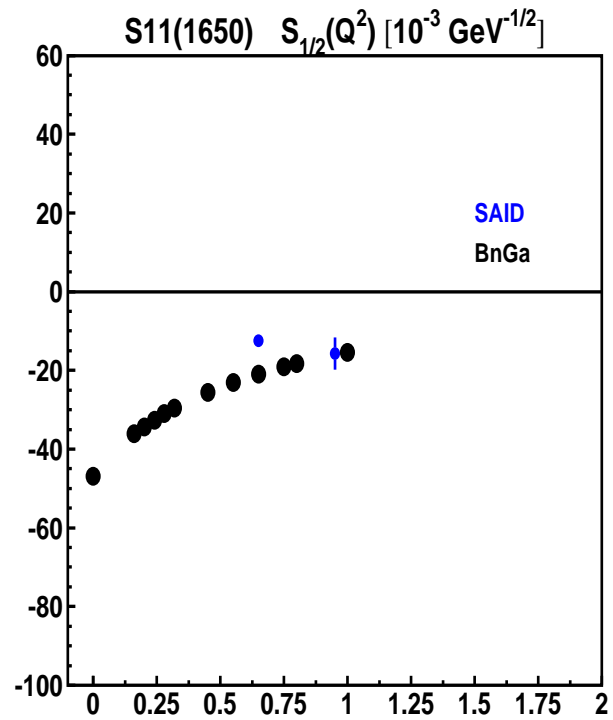
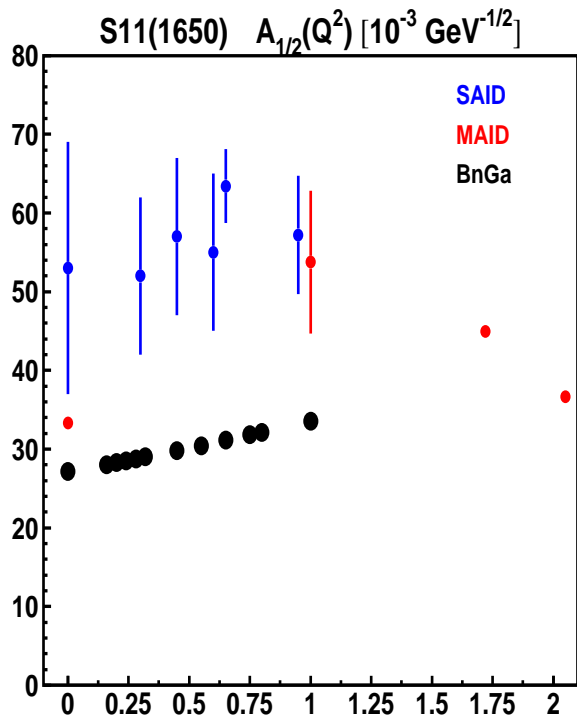
## The form factors for the $S_{11}(1535)$ state



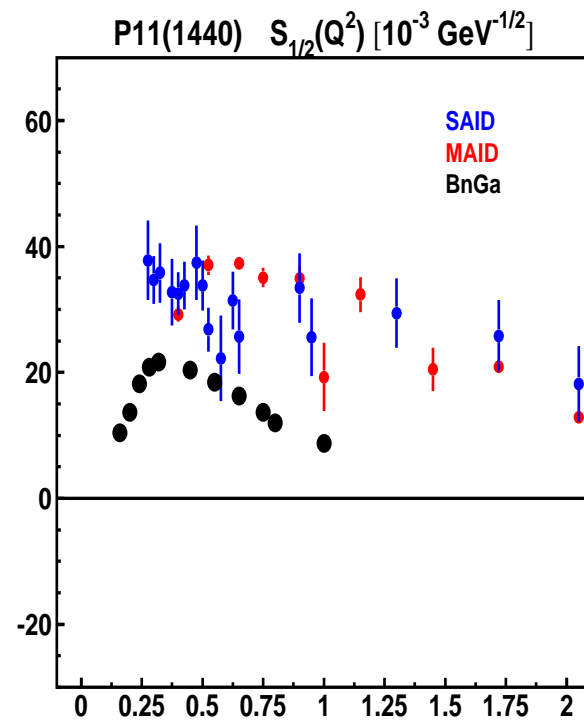
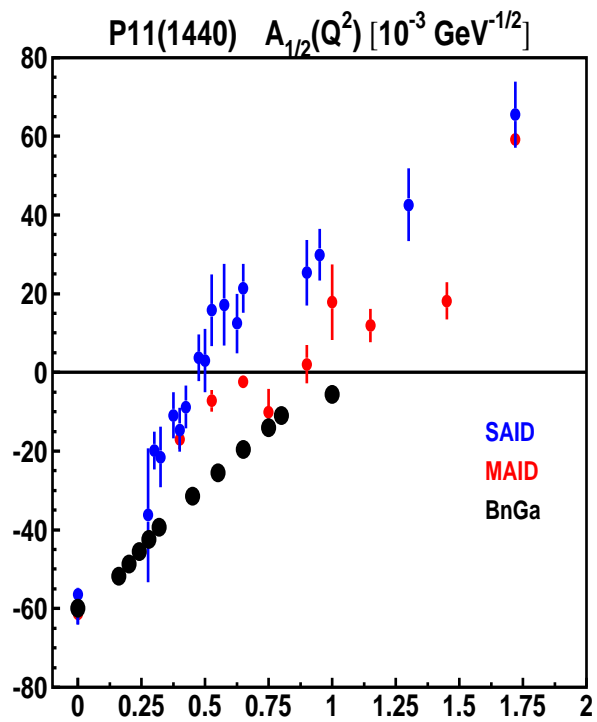
## The form factors for the $D_{15}(1675)$ state



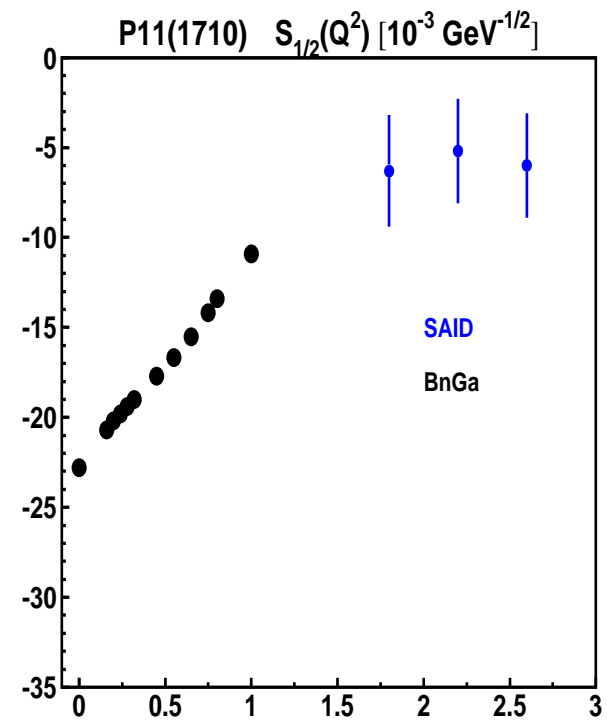
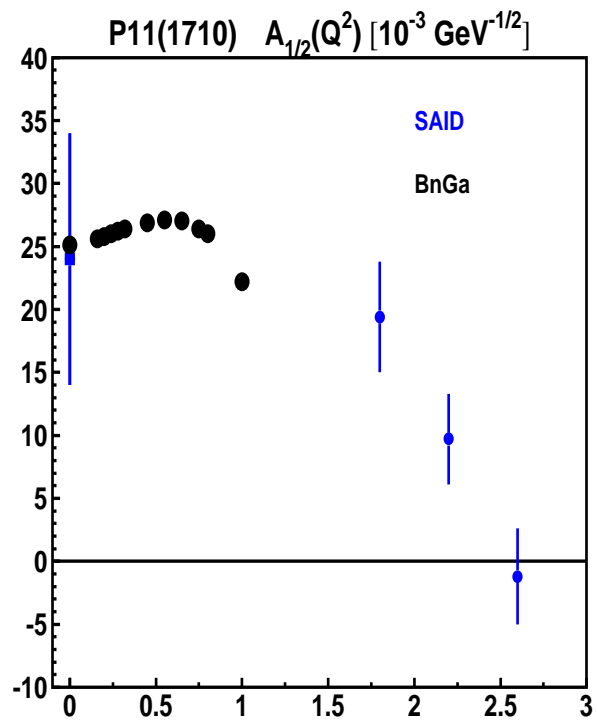
## The form factors for the $S_{11}(1650)$ state



## The form factors for the $P_{11}(1440)$ state



## The form factors for the $P_{11}(1710)$ state



## **SUMMARY**

- **The new BG2024 solution, which describes 208 data sets is obtained.**
- **The new polarization data on the double pion photoproduction provide an important constrain for the data analysis.**
- **The analysis of the electro-production data on the basis of latest solution is close to the finish line. But still there are some problems in the very low and very high mass region and error estimation is in progress.**
- **The combined analysis of the all single meson photo- and electro-production data is in progress.**